Astronomy & Astrophysics manuscript no. ms
(DOI: will be inserted by hand later)
February 5, 2008

arXiv:astro-ph/0510268v1 10 Oct 2005

The host galaxy/AGN connection in nearby early-type galaxies ⋆.

Is there a miniature radio-galaxy in every "core" galaxy?

Barbara Balmaverde[1] and Alessandro Capetti[2]

[1] Universitá di Torino, Via Giuria 1, I-10125, Torino, Italy
e-mail: `balmaverde@ph.unito.it`
[2] INAF - Osservatorio Astronomico di Torino, Strada Osservatorio 20, I-10025 Pino Torinese, Italy
e-mail: `capetti@to.astro.it`

Abstract. This is the second of a series of three papers exploring the connection between the multiwavelength properties of AGN in nearby early-type galaxies and the characteristics of their hosts. We selected two samples with 5 GHz VLA radio flux measurements down to 1 mJy, reaching levels of radio luminosity as low as 10^{36} erg s^{-1}. In Paper I we presented a study of the surface brightness profiles for the 65 objects with available archival HST images out of the 116 radio-detected galaxies. We classified early-type galaxies into "core" and "power-law" galaxies, discriminating on the basis of the slope of their nuclear brightness profiles, following the Nukers scheme. Here we focus on the 29 core galaxies (hereafter CoreG).

We used HST and Chandra data to isolate their optical and X-ray nuclear emission. The CoreG invariably host radio-loud nuclei, with an average radio-loudness parameter of Log R = L_{5GHz} / $L_B \sim 3.6$. The optical and X-ray nuclear luminosities correlate with the radio-core power, smoothly extending the analogous correlations already found for low luminosity radio-galaxies (LLRG) toward even lower power, by a factor of $\sim$ 1000, covering a combined range of 6 orders of magnitude. This supports the interpretation of a common non-thermal origin of the nuclear emission also for CoreG. The luminosities of the nuclear sources, most likely dominated by jet emission, set firm upper limits, as low as $L/L_{Edd} \sim 10^{-9}$ in both the optical and X-ray band, on any emission from the accretion process.

The similarity of CoreG and LLRG when considering the distributions host galaxies luminosities and black hole masses, as well as of the surface brightness profiles, indicates that they are drawn from the same population of early-type galaxies. LLRG represent only the tip of the iceberg associated with (relatively) high activity levels, with CoreG forming the bulk of the population.

We do not find any relationship between radio-power and black hole mass. A minimum black hole mass of $M_{BH} = 10^8 M_\odot$ is apparently associated with the radio-loud nuclei in both CoreG and LLRG, but this effect must be tested on a sample of less luminous galaxies, likely to host smaller black holes.

In the unifying model for BL Lacs and radio-galaxies, CoreG likely represent the counterparts of the large population of low luminosity BL Lac now emerging from the surveys at low radio flux limits. This suggests the presence of relativistic jets also in these quasi-quiescent early-type "core" galaxies.

Key words. galaxies: active, galaxies: bulges, galaxies: nuclei, galaxies: elliptical and lenticular, cD, galaxies: jets, (Galaxies:) BL Lacertae objects: general

1. Introduction.

The recent developments in our understanding of the nuclear regions of nearby galaxies provide us with a new framework in which to explore the classical issue of the connection between host galaxies and AGN.

All evidence now points to the idea that most galaxies host a supermassive black hole (SMBH) in their centers (e.g. Kormendy & Richstone 1995) and that its mass is closely linked to the host galaxies properties, such as the stellar velocity dispersion (Ferrarese & Merritt 2000; Gebhardt et al. 2000). This is clearly indicative of a coevolution of the galaxy/SMBH system and it also provides us with indirect, but robust, SMBH mass estimates for large sample of objects. Furthermore, the innermost structure of nearby galaxies have been revealed by HST imaging, showing the ubiquitous presence of singular starlight distribu-

---

Send offprint requests to: B. Balmaverde

⋆ Based on observations obtained at the Space Telescope Science Institute, which is operated by the Association of Universities for Research in Astronomy, Incorporated, under NASA contract NAS 5-26555.

tions with surface brightness diverging as $\Sigma(r) \sim r^{-\gamma}$ with $\gamma > 0$ (e.g. Lauer et al. 1995). The distribution of cusp slopes (Faber et al. 1997) is bimodal, with a paucity of objects with $0.3 < \gamma < 0.5$. Galaxies can then be separated on the basis of their brightness profiles in the two classes of “core” ($\gamma \leq 0.3$) and “power-law” ($\gamma \geq 0.5$) galaxies, in close correspondence to the revision of the Hubble sequence proposed by Kormendy & Bender (1996).

But despite these fundamental breakthroughs we still lack a clear picture of the precise relationship between AGN and host galaxies. For example, while spiral galaxies preferentially harbour radio-quiet AGN, early-type galaxies host both radio-loud and radio-quiet AGN. Similarly, radio-loud AGN are generally associated with the most massive SMBH as there is a median shift between the radio-quiet and radio-loud distribution, but both distributions are broad and overlap considerably (e.g. Dunlop et al. 2003).

In this framework, in two senses early-type galaxies appear to be the critical class of objects, where the transition between the two profiles classes occurs (i.e. in which core and power-law galaxies coexist) and in which they can host either radio-loud and radio-quiet AGN. We thus started a comprehensive study of a sample of early-type galaxies (see below for the sample definition) to explore the connection between the multiwavelength properties of AGN and the characteristics of their hosts. Since the ’Nuker’ classification can only be obtained when the nuclear region, potentially associated with a shallow cusp, can be well resolved, such a study must be limited to nearby galaxies. The most compact cores will be barely resolved at a distance of 40 Mpc (where 10 pc subtend $0\farcs05$) even in the HST images. Furthermore, high quality radio-images are required for an initial selection of AGN candidates.

We then examined two samples of nearby objects for which radio observations combining relatively high resolution, high frequency and sensitivity are available, in order to minimize the contribution from radio emission not related to the galaxy’s nucleus and confusion from background sources. More specifically we focus on the samples of early-type galaxies studied by Wrobel & Heeschen (1991) and Sadler et al. (1989) both observed with the VLA at 5 GHz with a flux limit of $\sim$ 1 mJy. The two samples were selected with a very similar strategy. Wrobel (1991) extracted a northern sample of galaxies from the CfA redshift survey (Huchra et al. 1983) satisfying the following criteria: (1) $\delta_{1950} \geq 0$, (2) photometric magnitude $B \leq 14$; (3) heliocentric velocity ≤ 3000 km s^{-1}, and (4) morphological Hubble type T$\leq$-1, for a total number of 216 galaxies. Sadler et al. (1989) selected a similar southern sample of 116 E and S0 with $-45 \leq \delta \leq -32$. The only difference between the two samples is that Sadler et al. did not impose a distance limit. Nonetheless, the threshold in optical magnitude effectively limits the sample to a recession velocity of $\sim$ 6000 km s^{-1}.

In Capetti & Balmaverde (2005, hereafter Paper I), we focused on the 116 galaxies detected in these VLA surveys to boost the fraction of AGN with respect to a purely optically selected sample. We used archival HST observations, available for 65 objects, to study their surface brightness profiles and to separate these early-type galaxies into core and power-law galaxies following the Nukers scheme, rather than on the traditional morphological classification (i.e. into E and S0 galaxies). Here we focus on the sub-sample formed by the 29 “core” galaxies.

We adopt a Hubble constant $H_o = 75$ km s^{-1} Mpc^{-1}.

2. A critical analysis of the classification as core galaxies.

In Paper I we adopted the classification into power-law and core galaxies following the scheme proposed by Lauer et al. (1995). We then separated early-type galaxies on the basis of the slope of their nuclear brightness profiles obtained using the Nukers law (i.e. a double power-law with innermost slope γ) defining as core-galaxies all objects with $\gamma \leq 0.3$. Since this strategy has been subsequently challenged by Graham et al. (2003), who introduced a different definition of core-galaxies, it is clearly important to assess whether the identification of an object as a core galaxy is dependent on the fitting scheme adopted.

Graham et al. argued that a Sérsic model (Sérsic 1968) provides a better characterization of the brightness profiles of early-type galaxies. In particular they pointed out that, among other issues, i) the values of the Nukers law parameters depend on the radial region used for the fit, ii) the Nukers fit is unable to reproduce the large scale behaviour of early-type galaxies and, most importantly for our purposes, iii) the identification of a core galaxy from a Nuker fit might not be recovered by a Sérsic fit. Conversely, they were able to fit power-law galaxies (in the Nukers scheme), as well as dwarf ellipticals (Graham & Guzmán 2003), with a single Sérsic law over the whole range of radii. They also suggested a new definition of core-galaxy as the class of objects showing a light deficit toward the center with respect to the Sérsic law (Trujillo et al. 2004).

In this context, we discuss in detail here the behaviour of the most critical objects, i.e. the two core galaxies for which the Nuker law returns the smallest values for the break radius, namely UGC 7760 and UGC 7797 for which $r_b = 0\farcs49$ and $r_b = 0\farcs21$ respectively. We fit both objects with a Sérsic law. The final fits, shown in Fig. 1, were obtained iteratively, fitting the external regions while flagging the innermost points out to a radius at which the residual from the Sérsic law exceeded a threshold of 5 %. The Sérsic law in general provides a remarkably good fit to the outer regions, with typical residuals of $\sim$ 1%, but a substantial central light deficit is clearly present in both objects. This indicates that both objects can be classified as core-galaxies in the Graham et al. scheme.

Using the brightness profiles for the core-galaxies for which we obtained Nuker fits in Paper I (14 additional objects) we obtained similar results. Very satisfactory fits can be obtained with a Sérsic law on the external regions of these galaxies, but they all show an even clearer central light deficit, as expected given the presence of well resolved shallow cores.

We conclude that, for the galaxies of our sample, the objects classified as core-galaxies in the Nuker scheme are recovered as such with the Graham et al. definition.

3. Basic data and nuclear luminosities

The basic data for the selected galaxies, namely the recession velocity (corrected for Local Group infall onto Virgo), the K band magnitude from the Two Micron All Sky Survey (2MASS), the galactic extinction and the total and core radio fluxes were given in Paper I.

In the following three subsections, we derive and discuss the measurements for the nuclear sources in the optical, X-ray and radio bands.

3.1. Optical nuclei.

The detection and measurement of an optical nuclear source at the center of a galaxy is a challenging task particularly when it represents only a small contribution with respect to the host emission, as is likely often to be the case of the weakly active galaxies making up our sample.

Different approaches have been employed in the literature. The most widely used method is to fit the overall brightness profile of a galaxy with an empirical functional form and to define a galaxy as "nucleated" when it shows a light excess in its central region with respect to the model (e.g. Lauer et al. 2004; Ravindranath et al. 2001). The drawback of this "global" approach is that it assumes that the model can be extrapolated inwards from the radial domain over which the fit was performed. Furthermore, the measurement and identification of the nuclear component are coupled with the behaviour of the brightness profile at all radii and with the specific choice of an analytic form. Although this is not a significant issue for bright point sources, it is particularly worrisome for the faint nuclei we are dealing with. Nonetheless, Rest et al. (2001) pointed out that in general nuclear light excesses are associated with a steepening of the profile as the HST resolution limit is approached. Indeed this is expected in the presence of a nuclear point source, since the convolution with the Point Spread Function produces a smooth decrease of the slope toward the center when only a diffuse galactic component is present. We therefore preferred to adopt a "local" approach to identify nuclear sources, based on the characteristic up-turn they cause in the nuclear brightness profile.

More specifically, we evaluated the derivative of the brightness profile in a log-log representation for the sources of our sample. In order to increase the stability of the slope measurement this has been estimated by combining the brightness measured over two adjacent points on each side of the radius of interest, yielding a second order accuracy. We then look for the presence of a nuclear up-turn in the derivative requiring for a nuclear detection a difference larger than 3 σ from the slopes at the local minimum and maximum. This a rather conservative definition since the region over which the up-turn is detected extends over several pixels while we only consider the peak-to-peak difference.

To illustrate this we focus on three cases. In the HST image as well as in the brightness profile of IC 4296 a nucleus clearly stands out against the underlying background and the central steepening at about $r = 0\farcs15$ is highly significant. NGC 4373 is the detection with the least significance of our sample, in which the presence of a nucleus is uncertain from just the visual inspection of the optical image, but the derivative of the brightness profile reveals the effect of the point source with an increase of 0.013 ± 0.004 from $r = 0\farcs1$ and $r = 0\farcs07$. Instead in NGC 1316 we do not have evidence for any compact point source, both in the image and in the brightness profile derivative, and it is considered as a non-detection.

Adopting this strategy in 18 out of 29 objects we identify an optical nucleus, with a percentage of $\sim 60\%$ of the total sample. In seven objects we did not find any upturn and these are considered upper limits. Note that this is again a conservative approach, since a nuclear source can still be present but its intensity might not be sufficient to compensate the downward trend of the derivative sets by the host galaxy.

In the remaining 4 objects the central regions have a complex structure and no estimate of the optical nucleus intensity can be obtained. In two cases (UGC 8745 and UGC 9723) the central regions are completely hidden by a kpc scale edge-on disk, while in NGC 3557 the study of its nuclear regions is hampered by the presence of a circumnuclear dusty disk. In UGC 9655, the innermost region ($r < 0\farcs1$) has a lower brightness than its surrounding; since only a single band image is available we cannot assess if this is due to dust absorption or to a genuine central brightness minimum as in the cases discussed by Lauer et al. (2002).

We measured the nuclear luminosity with the task RADPROF in IRAF, choosing as the extraction region a circle centered on the nucleus with radius set at the location of the up-turn and as the background region a circumnuclear annulus, $0.1''$ in width. For the undetected nuclei we set as upper limits the light excess with respect to the starlight background within a circular aperture $0.1''$ in diameter. Then we use the PHOTFLAM and EXPTIME keyword in the image header to convert the total counts to fluxes. Errors on the measurements of the optical nuclei are dominated by the uncertainty in the behaviour of the host's profile, while the statistical and absolute calibration errors amount to less than 10 %.h The very presence of the nucleus prevents us from determining accurately the host contribution within the central aperture. Our strategy is to remove the background measured as close as possible to the nucleus, i.e. effectively we adopted a constant starlight distribution in the innermost regions. An alternative approach would be to extrapolate the profile with

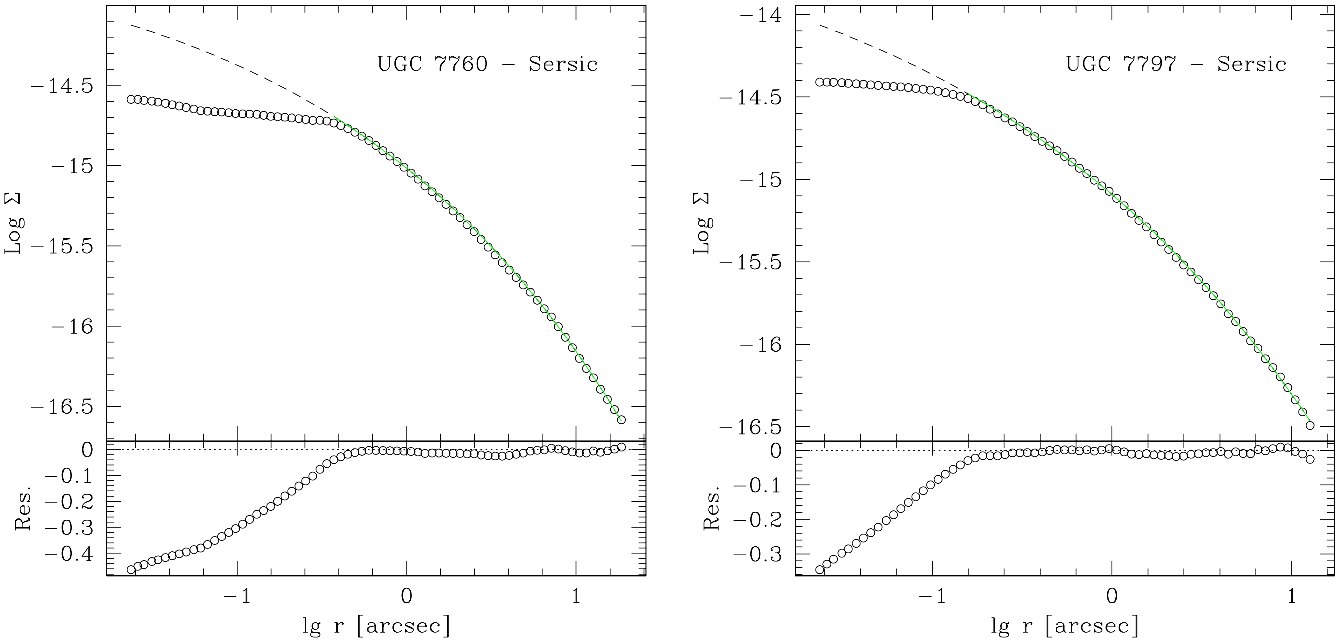

Fig. 1. Sérsic fits for the two core galaxies of our sample with the smallest values for the core radius. A substantial central light deficit is clearly present in both objects, conforming to the "core" classification in the Graham et al. scheme.

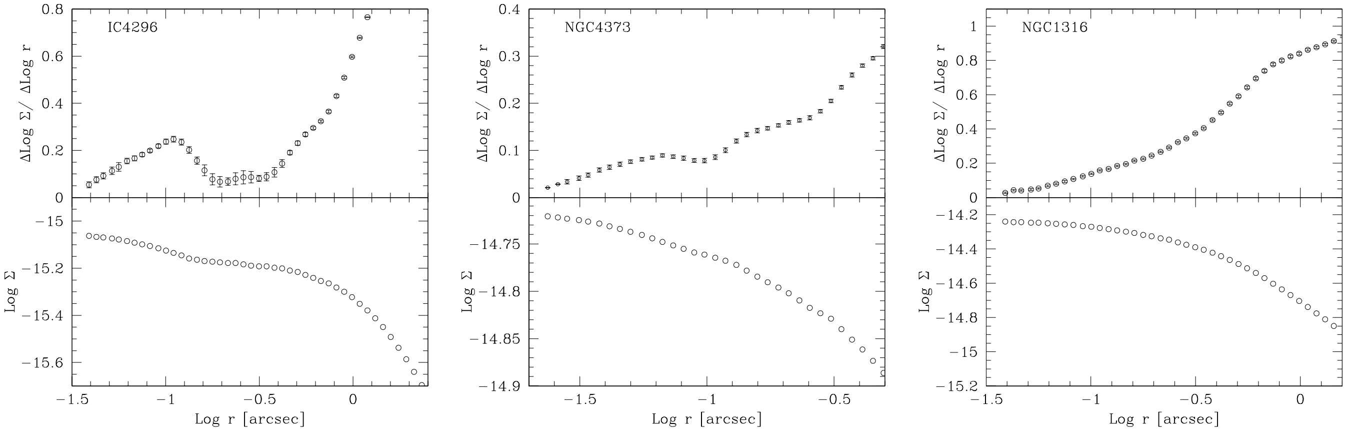

Fig. 2. Brightness profile and its derivative for three objects of the sample, namely IC 4296, NGC 4373 and NGC 1316. The first two galaxies show, at decreasing significance level, the characteristic up-turn in the profile associated with a nuclear source. This is not seen in the third object which is then considered as a non-detection.

a constant slope instead. Our definition of nuclear sources (an increase in the profile's derivative) implicitly requires that the observed profile lies above this extrapolation, but the resulting flux is reduced by at most a factor of 2 (with respect to the case of constant background) for the nuclei with the smallest contrast against the galaxy. As will become clear in the next sections, errors of this magnitude only have a marginal impact on our conclusions. The resulting fluxes are reported in Table 1. We finally derived all the luminosities referred to 8140 Å (see Table 2), after correcting for the Galactic extinction as tabulated in Paper I and adopting an optical spectral index[1] $\alpha_o = 1$.

3.2. X-ray nuclei

For the measurements of the X-ray nuclei we concentrate only on the Chandra measurements, as this telescope provides the best combination of sensitivity and resolution necessary to detect the faint nuclei expected in these

---

[1] We define the spectral index α with the spectrum in the form $F_\nu \propto \nu^{-\alpha}$

Table 1. (1) optical name (2) Chandra observational identification number, (3) exposure time [ks], (4) reference for the X-ray analysis (see below for the list), (5) instrument and filter of the HST observation, (6) optical nuclear flux [erg cm^{-2} s^{-1}].

Name	Chandra data summary			HST data summary	
	Obs. Id	Exp. time	Ref.	Image	F$_0$
UGC 0968	–	–	–	WFPC2/F814W	<4.0 E-14
UGC 5902	1587	31.9	(1)	WFPC2/F814W	<6.3 E-14
UGC 6297	2073	39.0	(1)	WFPC2/F814W	<5.0 E-14
UGC 7203	3995	5.13	(1)	WFPC2/F702W	4.0 E-14
UGC 7360	834	35.2	(2)	NICMOS/F160W	1.9 E-13
UGC 7386	398	1.43	(3)	NICMOS/F160W	1.6 E-13
UGC 7494	803	28.85	(2)	NICMOS/F160W	3.3 E-13
UGC 7629	321	40.1	(4)	WFPC2/F555W	1.4 E-14
UGC 7654	1808	14.17	(2)	NICMOS/F160W	5.1 E-12
UGC 7760	2072	55.14	(5)	WFPC2/F555W	6.8 E-14
UGC 7797	–	–	–	WFPC2/F702W	<1.0 E-13
UGC 7878	323	53.05	(4)	WFPC2/F814W	4.3 E-14
UGC 7898	785	37.35	(6)	WFPC2/F555W	<1.8 E-14
UGC 8745	–	–	–	WFPC2/F814W	–
UGC 9655	–	–	–	WFPC2/F702W	–
UGC 9706	4009	30.79	(5)	WFPC2/F702W	1.5 E-14
UGC 9723	2879	34.18	(7)	WFPC2/F814W	–
NGC 1316	2022	30.23	(8)	NICMOS/F160W	<9.6 E-13
NGC 1399	319	56.66	(4)	WFPC2/F814W	1.4 E-14
NGC 3258	–	–	–	ACS/F814W	4.9 E-14
NGC 3268	–	–	–	ACS/F814W	<1.5 E-14
NGC 3557	3217	37.99	(1)	WFPC2/F555W	–
NGC 4373	–	–	–	WFPC2/F814W	2.4 E-14
NGC 4696	1560	85.84	(9)	ACS/F814W	2.0 E-14
NGC 5128	463/1253	19.6+6.88	(10)	NICMOS/F222W	4.5 E-11
NGC 5419	4999/5000	15+15	(1)	WFPC2/F555W	6.7 E-14
IC 1459	2196	60.17	(11)	WFPC2/F814W	4.4 E-13
IC 4296	3394	25.4	(12)	NICMOS/F160W	9.5 E-14
IC 4931	–	–	–	WFPC2/F814 W	1.9 E-14

(1) this work, (2) Balmaverde & Capetti (2005), (3) Ho et al. (2001), (4) Loewenstein et al. (2001), (5) Filho et al. (2004), (6) Randall et al. (2004), (7) Terashima & Wilson (2003), (8) Kim & Fabbiano (2003), (9) Satyapal et al. (2004), (10) Evans et al. (2004), (11) Fabbiano et al. (2003), (12) Pellegrini et al. (2003).

weakly active galaxies. Data for 21 core galaxies are available in the Chandra public archive.

When available, we used the results of the analysis of the X-ray data from the literature. We find estimates of the luminosities of the nuclear sources (usually defined as the detection of a high energy power-law component) based on Chandra data for 16 objects of our sample (12 of which are detections and 4 are upper limits) which we rescaled to our adopted distance and converted to the 2-10 keV band, using the published power law index. In Tab 1 we give a summary of the available Chandra data, while references and details on the X-ray observations and analysis are presented in Appendix A.

We also considered the Chandra archival data for the 5 unpublished objects, namely UGC 5902, UGC 6297, UGC 7203, NGC 3557 and NGC 5419. We analyzed these observations using the Chandra data analysis CIAO v3.0.2, with the CALDB version 2.25, using the same strategy as in Balmaverde & Capetti (2005). We reprocessed all the data from level 1 to level 2, subtracting the bad pixels, applying ACIS CTI correction, coordinates and pha randomization. We searched for background flares and excluded some period of bad aspect.

We then extracted the spectrum in a circle region centered on the nucleus with a radius of 2″ and we take the background in an annulus of 4″. We grouped the spectrum to have at least 10 counts per bin and applied Poisson statistics.

For two objects (NGC 3557 and NGC 5419) we obtain a detection of a nuclear power-law source by fitting the spectrum using an absorbed power-law plus a thermal model, with the hydrogen column density fixed at the Galactic value. Details of the results are given in Appendix A. For the remaining 3 galaxies we set an upper limit to any nuclear emission, with the conservative hypothesis that all flux that we measure is non-thermal. We then fit the spectrum with an absorbed (to the galactic value) power law model with photon index $\Gamma = 2$.

The X-ray luminosities for all objects are given in Table 2.

3.3. Radio nuclei.

The radio data available for all objects of our sample are drawn from the surveys by Wrobel & Heeschen (1991) and Sadler et al. (1989), performed with the VLA at 5 GHz with a resolution of $\sim 5''$. Although these represent the most uniform and comprehensive studies of radio emission in early-type galaxies, they do not always have a resolution sufficient to separate the core emission from any extended structure. Sadler et al. (1989) argued that at decreasing radio luminosity there is a corresponding increase of the fractional contribution of the radio core.

To verify whether the VLA data overestimate the core flux, we searched the literature for radio core measurements obtained at higher resolution (and/or higher frequency) than our data. This would improve the estimate of the core flux density, avoiding the contribution of extended emission or spurious sources to the nuclear flux as well as revealing any radio structure. Better measurements, from VLBI data or from higher frequency/resolution VLA data, are available for most CoreG (23 out of 29) and compact cores were detected in all but 2 objects. The radio core fluxes are taken from Nagar et al. (2002) (15 GHz VLA data and 5 GHz VLBI data), Filho et al. (2002) and Krajnović & Jaffe (2002) (8.4 GHz at the VLA), Jones & Wehrle (1997) (8.4 GHz VLBI data) and Slee et al. (1994) (PTI 5 GHz interpolated data).

In Fig. 3 we compare the radio core flux density used in our analysis against observations made at higher resolution. Overall there is a substantial agreement between the two datasets, with a median difference of only ∼0.25 dex (a factor ∼1.6), with only two objects substantially offset (by a factor of ∼ 10). However, since these data are highly inhomogeneous and given the general agreement with the 5 GHz VLA measurements, we prefer to retain the values of Wrobel & Heeschen and Sadler et al.. Nonetheless, we always checked that using these higher resolution core fluxes our main results are not significantly affected (see Appendix B for a specific example).

4. The multiwavelength properties of nuclei of core galaxies.

Having collected the multiwavelength information for the nuclei of our core galaxies we can compare the emission in the different bands. First of all, we can estimate the ratio between the radio, optical and X-ray luminosities: the median values are $\mathrm{Log}(\nu L_r/\nu L_o) \sim -1.5$ (equivalent to a standard radio-loudness parameter Log R ∼ 3.6) [2] and $\mathrm{Log}\ \mathrm{R_X} = \mathrm{Log}(\nu L_\mathrm{r}/L_\mathrm{X}) \sim -1.3$, both with a dispersion of ∼ 0.5 dex. These ratios are clearly indicative of a radio-loud nature for these nuclei when compared to both the traditional separation into radio-loud and radio-quiet AGN (Log R = 1, e.g. Kellermann et al. 1994), as well as with the radio-loudness threshold introduced by Terashima & Wilson (2003) based on the X-ray to radio luminosity ratio (Log $\mathrm{R_X}$ = -4.5). Furthermore, the nuclear luminosities in all three bands are clearly correlated (see Fig. 4 and Table 3 for a summary of the results of the statistical analysis): the generalized (including the presence of upper limits) Spearman rank correlation coefficient ρ is 0.63 and 0.89 for L_r vs. L_o and L_r vs. L_X respectively, with probabilities that the correlations are not present of only 0.002 and 0.0001.

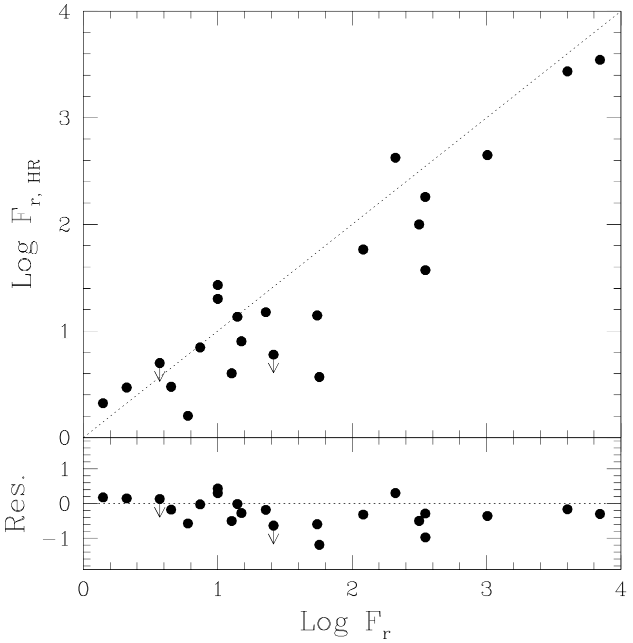

Fig. 3. Radio core flux density for CoreG obtained at 5 GHz with VLA (used in this work) compared to higher resolution data from Slee et al. (1994); Nagar et al. (2002); Filho et al. (2002); Krajnović & Jaffe (2002); Jones & Wehrle (1997). The dotted line is the bisectrix of the plane.

Both results are reminiscent of what is observed for the radio-loud nuclei of low luminosity radio-galaxies (LLRG). Chiaberge et al. (1999) and Balmaverde & Capetti (2005) reported on similar multiwavelength luminosity trends for the sample of LLRG formed by the 3C sources with FR I morphology. The connection between the CoreG and LLRG becomes more evident if we add LLRG in the diagnostic planes (see Fig. 5 and Table 4). The early-type core galaxies follow the same behaviour of the stronger radio galaxies, extending it downward by 3 orders of magnitude in radio-core luminosity as they reach levels as low as $L_\mathrm{r} \sim 10^{36}$ erg s^{-1}.

We estimated the best linear fit for the combined CoreG/LLRG sample in both the L_r vs. L_o and L_r vs. L_X planes. The best fits were derived as the bisectrix of the linear fits using the two quantities as independent variables following the suggestion by Isobe et al. (1990) that this is preferable for problems needing symmetrical treatment of the variables. The presence of upper limits in the independent variable suggests that we could take advantage of the methods of survival analysis proposed

---

[2] $\mathrm{R} = \mathrm{L_{5GHz}} / \mathrm{L_B}$. As in Sect. 3 we transformed the optical fluxes to the B band adopting an optical spectral index $\alpha_o = 1$.

Table 2. Core galaxies data: (1) UGC name, (2) intrinsic nuclear X-ray luminosity (2-10 keV) [erg s^{-1}], (3) nuclear optical luminosity (8140 Å)[erg s^{-1}] corrected for absorption using the galactic extinction values in Paper I, (4) nuclear radio luminosity (5GHz) [erg s^{-1}] derived from Paper I, (5) total radio luminosity (5GHz) [erg s^{-1}] derived from Paper I, (6) H_α+[NII] line luminosity [erg s^{-1}] from Ho et al. 1997 or ^{a} Phillips et al. 1986, (7) total K band galaxy's absolute magnitude from 2MASS, (8) logarithm of black hole mass in solar unity from ^{b} Marconi et al. 2003 or derived using the velocity dispertion.

Name	Log L_x	Log ν L_o	Log ν L_{core}	Log ν L_{tot}	Log $L_{H_\alpha+[NII]}$	M_K	Log $(M_{BH}/M_\odot)$
UGC 0968	–	<39.77	36.94	36.94	38.98	-25.39	8.54
UGC 5902	<38.40	<39.10	35.83	35.83	38.76	-24.25	8.00^b
UGC 6297	<38.40	<39.06	36.46	36.46	39.09	-23.40	8.33
UGC 7203	<38.93	39.85	37.44	37.44	38.74	-24.08	7.98
UGC 7360	40.95	39.71	39.22	40.64	39.76	-25.11	8.72^b
UGC 7386	39.72	38.76	38.38	38.38	39.60	-22.97	8.43
UGC 7494	39.30	39.27	38.57	39.48	39.14	-24.41	9.00^b
UGC 7629	38.23	38.79	37.73	37.95	37.98	-25.09	8.78
UGC 7654	40.30	40.72	39.90	41.15	40.00	-25.48	9.53^b
UGC 7760	38.40	38.73	37.30	37.3	37.90	-21.86	8.54
UGC 7797	–	<40.19	38.05	38.05	39.46	-24.61	8.33
UGC 7878	<38.41	39.07	36.90	37.77	38.60	-24.43	8.16
UGC 7898	<38.52	<39.13	37.46	37.59	–	-25.34	9.30^b
UGC 8745	–	Dusty	37.81	37.97	39.21	-25.07	8.39
UGC 9655	–	Dusty	36.96	36.96	39.01	-24.74	8.44
UGC 9706	38.26	39.25	37.31	37.31	39.11	-25.06	8.43
UGC 9723	<38.18	Dusty	36.92	36.92	38.28	-23.82	7.73
NGC 1316	39.62	<40.11	37.82	41.24	–	-25.99	8.36
NGC 1399	<38.79	38.65	37.20	38.73	–	-24.75	9.07
NGC 3258	–	39.91	37.42	38.57	–	-24.39	8.67
NGC 3268	–	<39.42	38.21	38.21	39.67^a	-24.55	8.33
NGC 3557	40.08	Dusty	37.94	39.41	–	-25.70	8.67
NGC 4373	–	39.79	38.15	38.15	–	-25.51	8.49
NGC 4696	40.04	39.59	38.65	40.05	39.30	-25.69	8.55
NGC 5128	42.11	40.31	39.05	40.31	38.16	-24.64	8.38^b
NGC 5419	40.69	40.79	38.42	39.83	–	-26.14	9.02
IC 1459	40.56	40.33	39.38	39.38	40.02^a	-24.70	9.18^b
IC 4296	41.18	39.85	39.46	40.35	39.74^a	-25.91	9.04
IC 4931	–	40.19	37.51	37.51	–	-25.79	8.67

by e.g. Schmitt (1985). However, the drawbacks discussed by Sadler et al. (1989) and, in our specific case, the non-random distribution of upper limits, argue against this approach. We therefore preferred to exclude upper limits from the linear regression analysis. Nonetheless, a posteriori, 1) the objects with an undetected nuclear component in the optical or X-ray are consistent with the correlation defined by the detections only; 2) the application of the Schmidt methods provides correlation slopes that agree, within the errors, with our estimates.

We obtained (indicating the Pearson correlation coefficient with r and slope with m) r_{ro}=0.90 and $m_{ro} = 0.89 \pm 0.07$, r_{rx}=0.89 $m_{rx} = 1.02 \pm 0.10$ for the radio/optical and radio/X-ray correlations respectively. The slopes and normalizations derived for CoreG, LLRG and the combined CoreG+LLRG sample (see Table 3) are consistent within the errors and this indicates that there is no significant change in the behaviour between the two samples. Only the dispersion is slightly larger for the CoreG nuclei being a factor of ~ 4 rather than ~ 2 for the LLRG sample alone.

Chiaberge et al. (1999) first reported the presence of a correlation between radio and optical emission in the LLRG and they concluded that this is most likely due to a common non-thermal jet origin for the radio and optical cores. Recently Balmaverde & Capetti (2005) extended the analysis to the X-ray cores; the nuclear X-ray luminosity also correlates with those of the radio cores and with a much smaller dispersion ($\sim$ 0.3 dex) when compared to similar trends found for other classes of AGN (see e.g. Falcke et al. 1995), again pointing to a common origin for the emission in the three bands. Furthermore, the broad band spectral indices of the 3C/FR I cores are very similar to those measured in BL Lacs objects (for which a jet origin is well established) in accord with the FR I/BL Lacs unified model (we will return to this issue in Section 7).

The core galaxies of our sample thus appear to smoothly extend the results obtained for LLRG to much lower radio luminosity, expanding the multiwavelenght nuclear correlations to a total of 6 orders of magnitude. This strongly argues in favour of a jet origin for the nuclear

Table 3. Correlations summary

Sample	Var. A	Var. B	r_{AB}	Slope	rms
CoreG	L_O	L_r	0.59	0.76±0.21	0.62
	L_X	L_r	0.78	1.36±0.20	0.59
LLRG	L_O	L_r	0.94	0.82±0.11	0.32
	L_X	L_r	0.95	0.99±0.11	0.33
LLRG+CoreG	L_O	L_r	0.90	0.89±0.07	0.56
	L_X	L_r	0.89	1.02±0.10	0.58

emission also in the core galaxies and that they simply represent the scaled down versions of these already low luminosity AGN.

4.1. Core galaxies vs. low luminosity radio-galaxies.

The results presented above indicate that the nuclei of the CoreG show a very similar behaviour to those of LLRG. Here we explore in more detail how CoreG and LLRG compare in their other properties, such as the structure of the host, black hole mass, radio-morphology and optical spectra.

Our sample was selected to include only early-type galaxies with a core profile, e.g. with an asymptotic slope (toward the nucleus) of their surface brightness profiles $\gamma < 0.3$. Recently de Ruiter et al. (2005) showed, from the analysis of a combined sample of B2 and 3C sources, that they are all hosted by early-type galaxies and that the presence of a flat core is a characteristic of the host galaxies of all nearby radio-galaxies.

A strong similarity between CoreG and LLRG emerges when comparing the mass of their supermassive black holes. When no direct measurement (taken from the compilation by Marconi & Hunt 2003) was available, we estimated M_{BH} using the relationship with the stellar velocity dispersion (taken from the LEDA database) in the form given by Tremaine et al. (2002). The distributions of M_{BH} (see Fig. 6) of the two samples are almost indistinguishable[3], as they have median values of Log $M_{BH} = 8.54$ and Log $M_{BH} = 8.70$, for CoreG and LLRG respectively, and they also cover the same range, with most objects with Log $M_{BH} = 8 - 9.5$.

Further indications of the nature of CoreG cores and their connection with LLRG come from the emission lines in their optical spectra. LLRG are characterized as a class by their LINER spectra (e.g. Lewis et al. 2003) and this is the case also for the CoreG of our sample. In the NED database, although about half of the CoreG do not have a spectral classification, 13 objects are classified as LINERs[4]. The only exception is UGC 7203, with a Seyfert spectrum, but its diagnostic line ratios are borderline with those of LINERs (Ho et al. 1997). Concerning the emission line luminosity, Capetti et al. (2005) found a tight relationship between radio core and line luminosity studying a group of LLRG formed by the 3C/FR I complemented by the sample of 21 radio-bright ($F_r > 150$ mJy) UGC galaxies defined by Noel-Storr et al. (2003). Line luminosity for our CoreG clearly follow the same trend defined by LLRG, although with a substantially larger dispersion, not unexpected given their low line luminosity and the non uniformity of the data used for this analysis.

Considering the radio structure, several objects of our CoreG sample have a radio-morphology with well developed jets and lobes: UGC 7360, UGC 7494 and UGC 7654 are FR I radio-galaxies part of the 3C sample (3C 270, 3C 272.1 and 3C 274), while in the Southern sample we have the well studied radio-galaxies NGC 1316 (Fornax A), a FR II source, NGC 5128 (Cen A) and IC 4296. A literature search shows that at least another 11 sources have extended radio-structure indicative of a collimated outflow, although in several cases this can only be seen in high resolution VLBI images, such as the mas scale double-lobes in UGC 7760 or the one-sided jet of UGC 7386 (Nagar et al. 2002; Falcke et al. 2000).

Conversely, hosts of 3C/FR I radio-sources are on average more luminous than core-galaxies (see Fig. 6, left panel) although there is a substantial overlap between the two groups: the median values are $M_K = -24.8$ and $M_K = -25.7$ for CoreG and 3C/FR I respectively, with a KS probability of only 0.003 of being drawn from the same population. This reflects the well known trend, already noted by Auriemma et al. (1977), for which a brighter galaxy has a higher probability of being a stronger radio emitter, and which is present also in our sample (Paper I). The selection of relatively bright radio sources, such as the 3C/FR I, corresponds to a bias toward more luminous galaxies. Indeed, within our sample, imposing a threshold in total radio-luminosity of $L_{\rm tot} > 10^{39}$ erg/s,[5] the low end for LLRG, decreases the median magnitude to -25.1, in closer agreement with the 3C/FR I value.

We conclude that the properties of our low radio luminosity CoreG show a remarkable similarity to those of classical LLRG, in particular, they share the presence of a flat core in their host's brightness profiles, they have the same distribution in black hole masses, as well as analogous properties concerning their optical emission lines and radio-morphology. These results indicate that core galaxies and LLRG can be considered, from these different point of view, as being drawn from the same population of early-type galaxies. They can only be separated on the basis of their different level of nuclear activity, with the LLRG forming the tip of the iceberg of (relatively) high luminosity objects. Furthermore, the emission processes asso-

---

[3] The probability that the two samples are drawn from the same parent distribution is 0.32, according to the Kolmogorov-Smirnoff test.

[4] This result provides further support to the suggestion by Chiaberge et al. (2005) that a dual population is associated with galaxies with a LINER spectrum, being formed by both radio-quiet and by radio-loud objects. The CoreG are part of this latter sub-population of radio-loud LINER.

[5] The 5 GHz luminosity was converted to 178 MHz for consistency with the 3C/FR I values adopting a spectral index of 0.7.

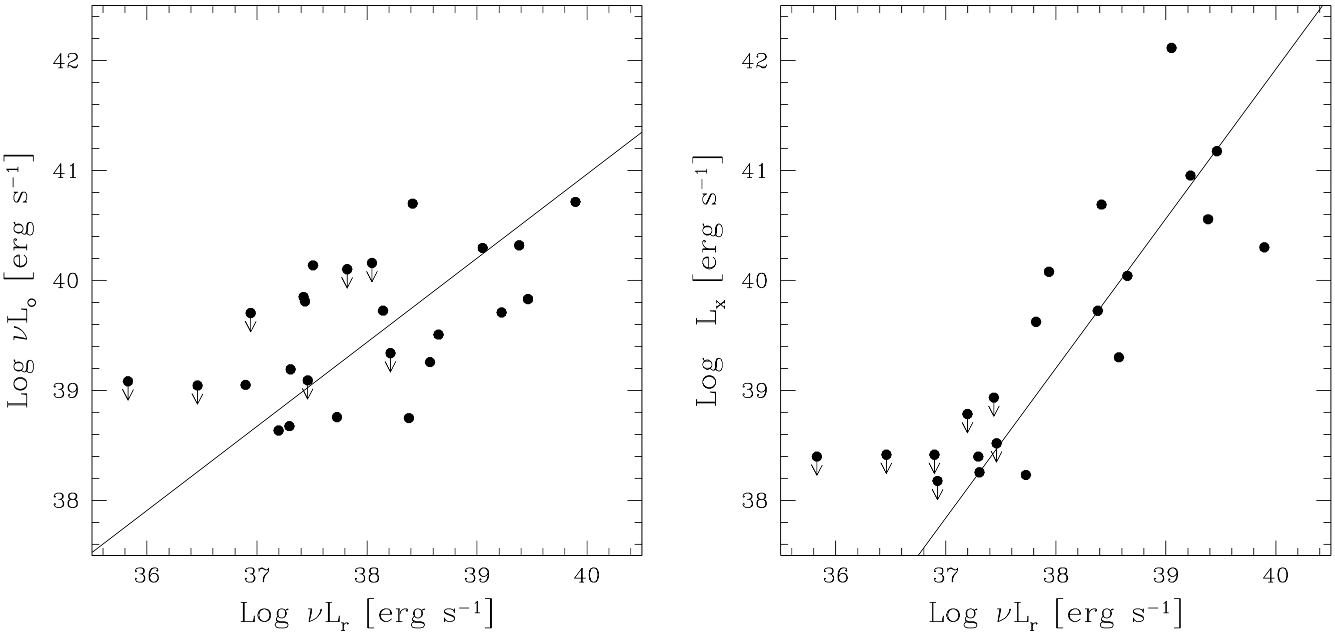

Fig. 4. Radio core luminosity for the early-type galaxies with a “core” profile versus the optical (left) and X-ray (right) nuclear luminosities.

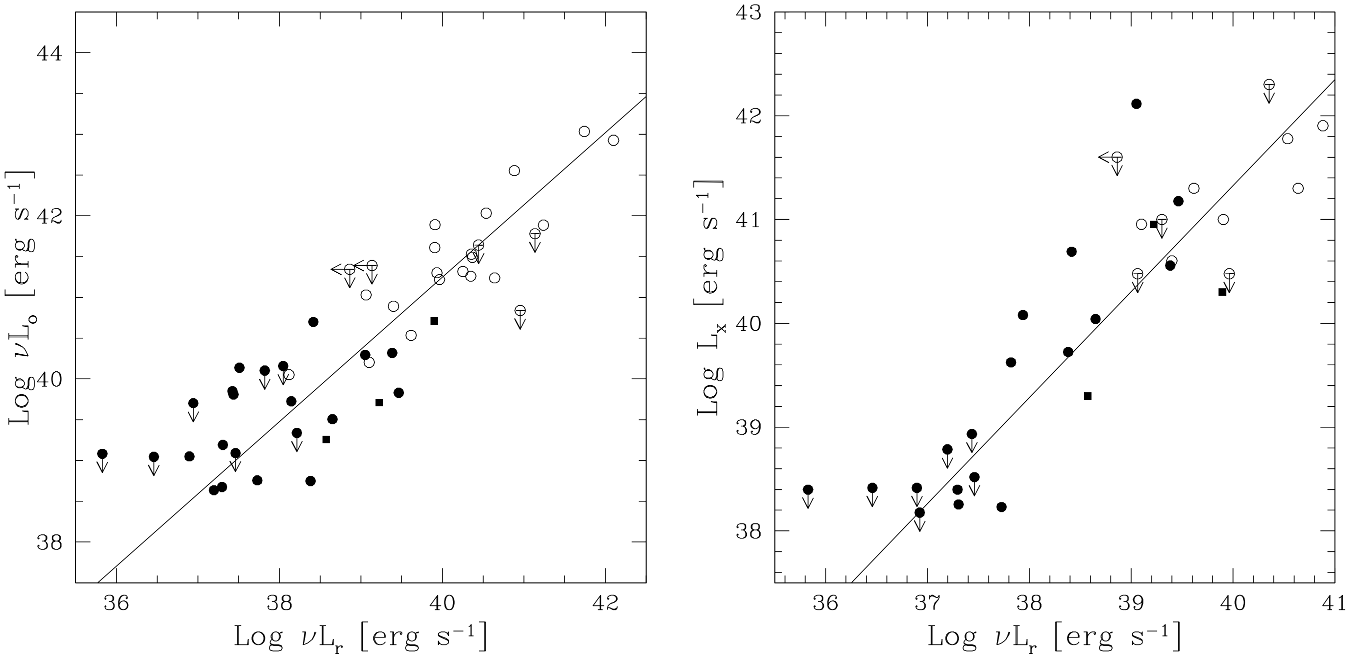

Fig. 5. Comparison of radio and optical (left) and X-ray (right) nuclear luminosity for the sample of core-galaxies (filled circles) and for the reference 3C/FR I sample of low luminosity radio-galaxies (empty circles). The three sources in common are marked with a filled square. The solid lines reproduce the best linear fits.

ciated to their activity scale almost linearly over 6 orders of magnitude in all bands for which data are available.

5. Black hole mass and radio luminosity.

The issue of the relationship between the black hole mass and the radio-luminosity has been discussed by several authors, taking advantage of the recent possibility to measure (or at least estimate) M_{BH}. Franceschini et al. (1998) pioneered this field showing, from a compilation of ob-

Table 4. Radio galaxies of the 3C/FR I sample data: (1) name, (2) intrinsic nuclear X-ray luminosity (2-10 keV) [erg s^{-1}], (3) nuclear optical luminosity (8140 Å)[erg s^{-1}], (4) nuclear radio luminosity (5GHz)[erg s^{-1}] and (5) total radio luminosity (178MHz)[erg s^{-1}] from Chiaberge et al. 1999, (6) H$_\alpha$+[NII] line luminosity from Capetti et al. 2005 [erg s^{-1}], (7) total K band galaxy's absolute magnitude from 2MASS, (8) logarithm of black hole mass in solar unity derived using the velocity dispertion or from ^{a} Marconi et al. 2003.

Name	Log L$_x$	Log ν L$_o$	Log ν L$_{core}$	Log ν L$_{tot}$	Log $L_{H_\alpha+[NII]}$	M_K	Log $(M_{BH}/M_\odot)$
3C 028	<41.60	<41.35	<38.86	42.32	–	-26.06	–
3C 029	–	41.32	40.25	41.01	40.40	-25.72	-8.11
3C 031	40.60	40.89	39.40	40.21	39.89	-25.67	-8.70
3C 066B	41.00	41.61	39.90	40.59	40.22	–	–
3C 075	< 41.00	–	39.30	40.28	–	–	8.84
3C 076.1	–	–	–	40.64	–	–	8.88
3C 078	41.90	42.55	40.88	40.74	40.71	-26.24	8.61
3C 083.1	40.95	40.2	39.10	40.75	39.26	–	–
3C 084	42.60	42.93	42.10	40.63	–	-26.11	8.58
3C 089	–	<40.84	40.95	42.12	–	-26.05	8.85
3C 189	41.78	42.03	40.54	42.80	–	–	–
3C 264	–	41.89	39.91	40.57	40.02	-25.09	8.67
3C 270	40.95	39.71	39.22	41.27	39.54	-25.11	8.72^a
3C 272.1	39.30	39.26	38.57	40.10	38.56	-24.41	9.00^a
3C 274	40.30	40.71	39.90	41.78	39.15	-25.48	9.53^a
3C 277.3	–	41.30	39.93	41.35	40.51	-25.20	–
3C 288	–	41.89	41.24	42.59	–	–	–
3C 293	–	–	40.29	40.94	–	-25.44	8.14
3C 296	41.30	40.53	39.62	40.39	–	–	8.80
3C 305	–	–	39.68	40.96	–	-25.45	8.07
3C 310	–	41.26	40.35	41.74	–	–	8.21
3C 314.1	–	<41.39	<39.14	41.71	–	–	–
3C 315	–	–	41.23	41.85	–	–	–
3C 317	41.30	41.24	40.64	41.27	–	-26.13	8.32
3C 338	< 40.48	41.22	39.96	41.16	40.54	–	8.92
3C 346	43.30	43.03	41.74	41.99	41.41	-26.32	–
3C 348	<42.30	41.53	40.36	43.45	–	-26.40	–
3C 424	–	<41.64	40.44	41.88	–	–	–
3C 433	–	–	39.69	42.29	–	–	–
3C 438	<42.60	<41.78	41.14	43.12	–	-27.00	–
3C 442	–	40.05	38.12	40.57	39.72	–	–
3C 449	<40.48	41.03	39.06	40.11	39.50	–	8.54
3C 465	–	41.49	40.37	41.06	40.72	–	9.14

jects with available black hole estimates, that the radio-luminosity tightly correlates with the black hole mass, with a logarithmic index of ~ 2.5. This result was subsequently challenged, by e.g. Ho (2002). We here re-explore this issue limiting ourselves to the sample of core early-type galaxies; while this substantially restricts the accessible range in M_{BH} and it applies only to radio-loud nuclei, it has the substantial advantage of performing the analysis on a complete sample with well defined selection criteria and covering a large range of radio-luminosity.

The comparison of the radio-core luminosity with the black hole mass is presented in Fig. 8. Apparently, a dependence of L_r on M_{BH} is present, although with a substantial scatter. However, the radio flux limit of the samples exclude objects with lower radio luminosity, potentially populating the lower part of the L_R vs. M_{BH} plane. Furthermore, the inclusion of LLRG (which, as discussed above, represent the high activity end of the early-type population) radically changes the picture, as they populate the whole upper portion of this plane. This indicates that a very large range (at least 4 orders of magnitude) of radio-power can correspond to a given M_{BH} [6]. This is a clear indication that, not unexpectedly, parameters other than the black hole mass play a fundamental role in determining the radio luminosity of a galaxy.

More notable is the lack of sources with $M_{BH} < 10^8 M_\odot$ (with only one exception). The effects produced by our selection criteria must be considered before any conclusion can be drawn. In particular the correlation between the black hole mass and the spheroidal galactic component, combined with the limiting magnitude, translates into a threshold in the accessible range of black

---

[6] With respect to previous studies we report the nuclear radio emission only, instead of the total radio luminosity. However, since the fraction of extended emission grows with radio luminosity, using the total power would just move the LLRG upward, further increasing the spread.

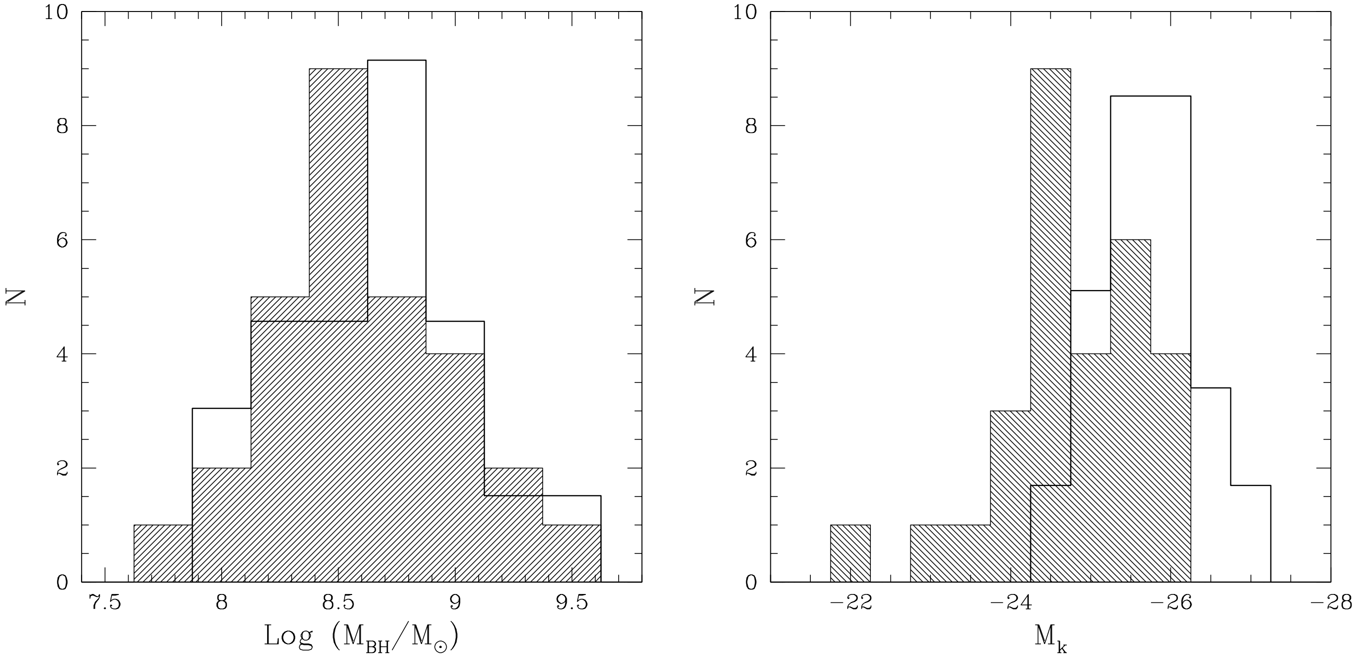

Fig. 6. Distributions for CoreG (shaded histograms) and for LLRG (empty histogram) of (left panel) black hole mass M_{BH} and (right panel) absolute magnitude M_K. The LLRG histograms have been re-normalized multiplying by a factor 29/19 for M_{BH} and 29/17 for M_K respectively, i.e. the number of objects in the two samples for which estimates of these parameters are available.

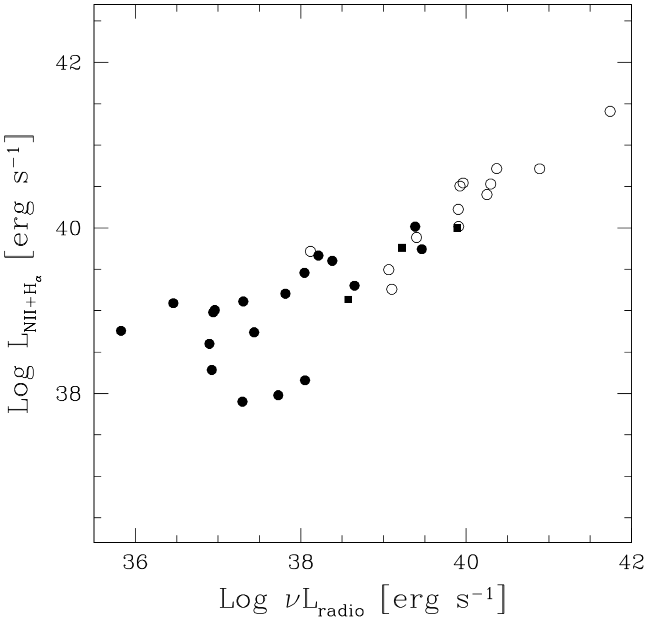

Fig. 7. Emission line vs. radio core luminosity for CoreG galaxies (filled circles) and for the LLRG 3C/FR I sample (empty circles), from Capetti et al. (2005).

hole masses. Using the limit in apparent magnitude of our sample ($m_B < 14$), an average color of B-K = 4.25 (Mannucci et al. 2001) and the best fit to the relationship between M_{BH} and M_K from Marconi & Hunt (2003) we obtain that at distances larger than 20 Mpc (corresponding to 7/8 of the volume covered in the Wrobel's sample) we do include galaxies with expected black hole masses $M_{BH} < 10^8 M_\odot$. This represents a severe bias against the inclusion of galaxies with low values of M_{BH}, regardless of their radio emission. The lack of low black hole mass LLRG seems to favour the reality of this effect, as they are not directly selected imposing an optical threshold; however, the already discussed statistical trend linking radio and optical luminosity might represent a more subtle bias leading to the same effect. The existence of a minimum black hole mass to produce a radio-loud nucleus must be properly tested extending the analysis to a sample of less luminous galaxies, likely to harbour less massive black holes.

6. Constraints on the radiative manifestation of the accretion process

Taking advantage of the estimates of black hole mass we can convert the measurements of the nuclear luminosities to units of the Eddington luminosity. All CoreG nuclei are associated with a low fraction of $L_{\rm Edd}$, being confined to the range $L/L_{\rm Edd} \sim 10^{-6} - 10^{-9}$ in both the X-ray and optical bands (with only one X-ray exception), see Fig. 9. Furthermore, as discussed in Sect. 4, the tight correlations between radio, optical and X-ray nuclear luminosities extending across LLRG and CoreG strongly argue in favour of a jet origin for the nuclear emission also in the core galaxies. If this is indeed the case, the observed nuclear

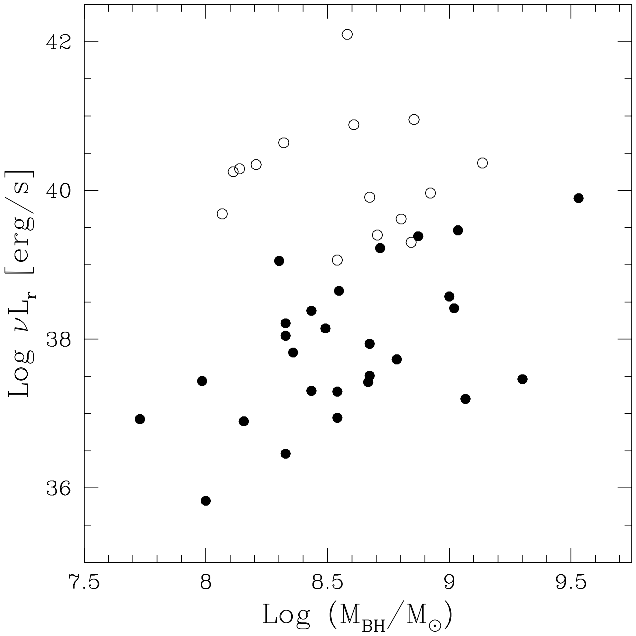

Fig. 8. Nuclear radio-luminosity vs. black hole mass M_{BH} for CoreG galaxies (filled circles) and for the LLRG 3C/FR I sample (empty circles).

emission does not originate in the accretion process and the values reported above should be considered as upper limits.

Our results add to the already vast literature reporting emission corresponding to a very low Eddington fraction associated with accretion onto supermassive black holes. These results prompted the idea that in these objects accretion occurs not only at a low rate but also at a low radiative efficiency, such as in the Advection Dominated Accretion Flows (ADAF, Narayan & Yi 1995) in which most of the gravitational energy of the accreting gas is advected into the black hole before it can be dissipated radiatively, thus reducing the efficiency of the process with respect to the standard models of geometrically thin, optically thick, accretion disks. The ADAF models have been rather successful in modeling the observed nuclear spectrum in several galaxies, such as e.g. the Galactic Center and NGC 4258 (Narayan & Yi 1995; Lasota et al. 1996). Conversely, ADAF models substantially over-predict the observed emission in the nuclei of nearby bright elliptical galaxies (Di Matteo et al. 2000; Loewenstein et al. 2001).

This suggested the possibility that a substantial fraction of the mass included within the Bondi's accretion radius (Bondi 1952) might not actually reach the central object, thus further reducing the radiative emission from the accretion process with respect to the ADAF models. This may be the case in the presence of an outflow (Advection Dominated Inflow/Outflow Solutions, or ADIOS, Blandford & Begelman 1999) or strong convection (Convection Dominated Accretion Flows, or CDAF, Quataert & Gruzinov 2000) in which most gas circulates in convection eddies rather than accreting onto the black hole.

Unfortunately, in the case of the galaxies under investigation, the comparison of the theoretical predictions with the observations so as to get constraints on the properties of the accretion process is quite difficult. This is due to the presence of different competing models, all of these with several free parameters, and to the observational data, in particular to the scarce multiwavelength coverage of the nuclear emission measurements which prevents us from deriving a detailed Spectral Energy Distribution of these objects. As discussed above, this is more complicated for our radio-loud nuclei in which the emission is most likely dominated by the non-thermal radiation from their jets.

Nonetheless, Pellegrini (2005) recently studied in detail a sample of nearby galaxies for which the Chandra observations provide an estimate of the temperature and density of the gas in the nuclear regions, thus enabling one to derive the expected Bondi accretion rate, $\dot{M}_B$. It is interesting to note that the estimates of $\dot{M}_B$ for three sources common to both samples with the lowest X-ray luminosity (namely NGC 1399, UGC 7629 (AKA NGC 4472) and UGC 7898 (AKA NGC 4649)) are relatively large, $\dot{M}_B/\dot{M}_{\rm Edd} = 10^{-2} - 10^{-4}$, while their X-ray luminosities are $L_X/L_{Edd} = 10^{-8} - 10^{-10}$ (see her Fig. 3). These luminosities are between 3 and 5 orders of magnitude lower than expected from an ADAF model, and they should be considered only as upper limits. These results argue in favour of an effective accretion rate substantially smaller than expected in the case of spherical accretion, suggesting that an important role is played by mass loss due to an outflow or by convection.

7. CoreG and the BL Lacs/LLRG unifying model

In Section 4.1 we presented evidence that "core" galaxies and LLRG are drawn from the same population of early-type galaxies. They can only be separated on the basis of their different level of nuclear activity, with CoreG representing the low luminosity extension of LLRG. The CoreG nuclei appear to be the scaled down versions of those of LLRG when their multiwavelength nuclear properties are considered. Thus here we are sampling a new regime for radio-galaxies in terms of nuclear power and it is important to explore the implications of this result for the model unifying BL Lac objects and radiogalaxies.

Unification models ascribe the differences between the observed properties of different classes of AGN to the anisotropy of the nuclear radiation (see e.g. Antonucci 1993; Urry & Padovani 1995, for reviews). In particular, for low luminosity radio-loud objects, it is believed that BL Lac objects are the pole-on counterparts of radio-galaxies, i.e. their emission is dominated by the radiation from the inner regions of a relativistic jet seen at a small angle from its axis which is thus strongly amplified by relativistic Doppler beaming. In FR I, whose jets are observed at larger angles with respect to the line of sight, the nuclear component is strongly de-amplified. Contrary

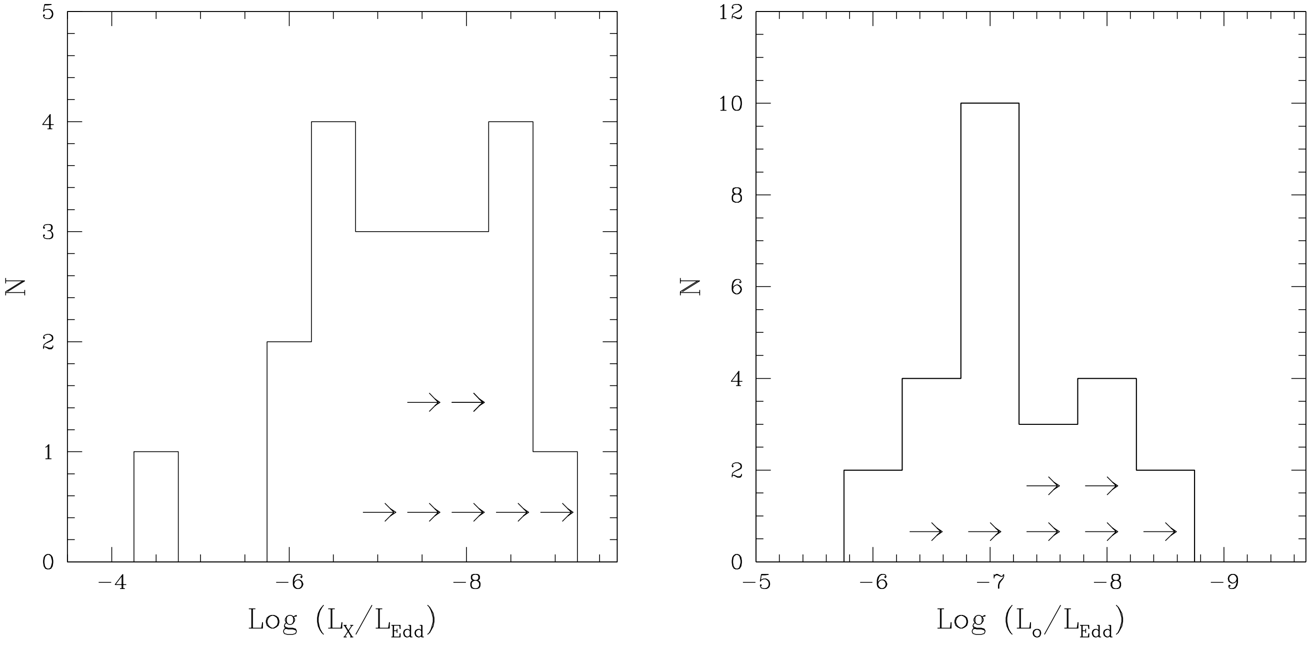

Fig. 9. Distributions of the nuclear luminosities measured as fraction of the Eddington luminosity in the X-ray (left) and optical (right) bands.

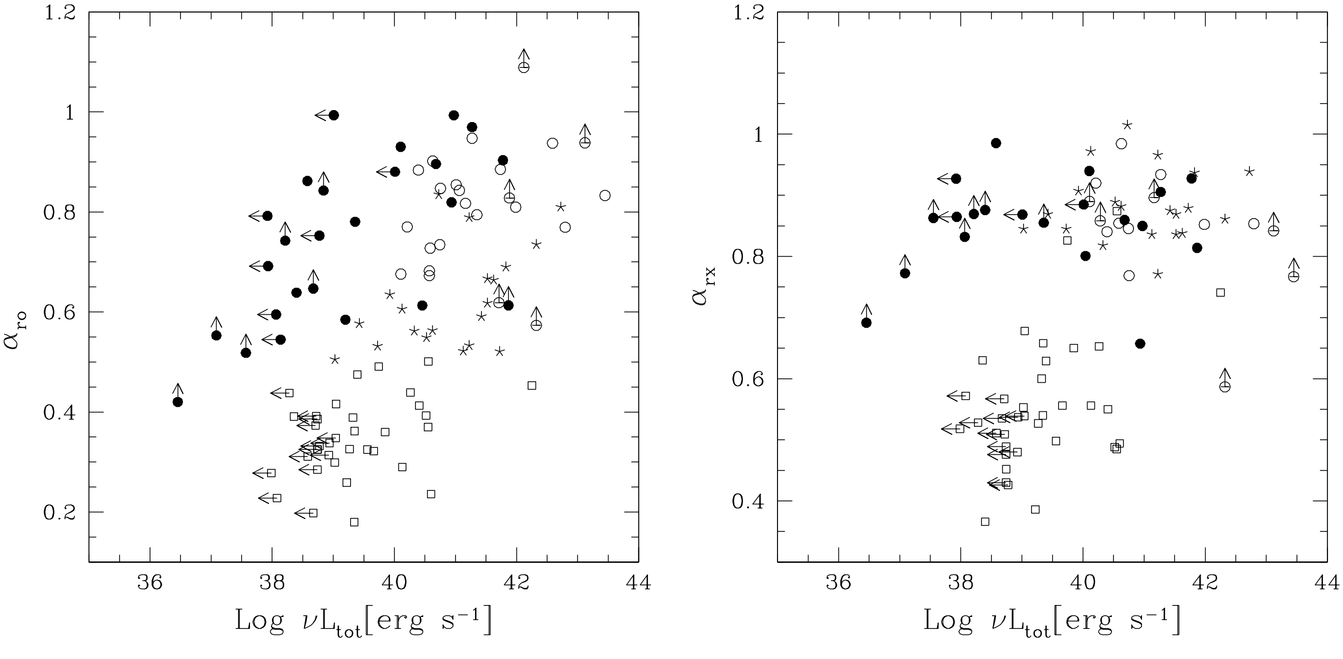

Fig. 11. Broad band spectral indices vs. extended radio luminosity for core galaxies (filled circles), LLRG (empty circles), LBL (stars) and HBL (squares). The CoreG luminosity has been extrapolated to 178 MHz adopting a spectral index of 0.7.

to other classes of AGN there is growing evidence that obscuration does not play a significant role in these objects (Henkel et al. 1998; Chiaberge et al. 1999; Donato et al. 2004; Balmaverde & Capetti 2005).

Balmaverde & Capetti (2005) found that there is a close similarity of the broad band spectral indices between LLRG and the sub-class of the BL Lacs, the Low energy peaked BL Lac (LBL, Padovani & Giommi 1995), in agreement with the unified model[7]. We performed the

---

[7] The small offsets between the two classes can be quantitatively accounted for by the effects of beaming since Doppler beaming not only affects the angular pattern of the jet emis-

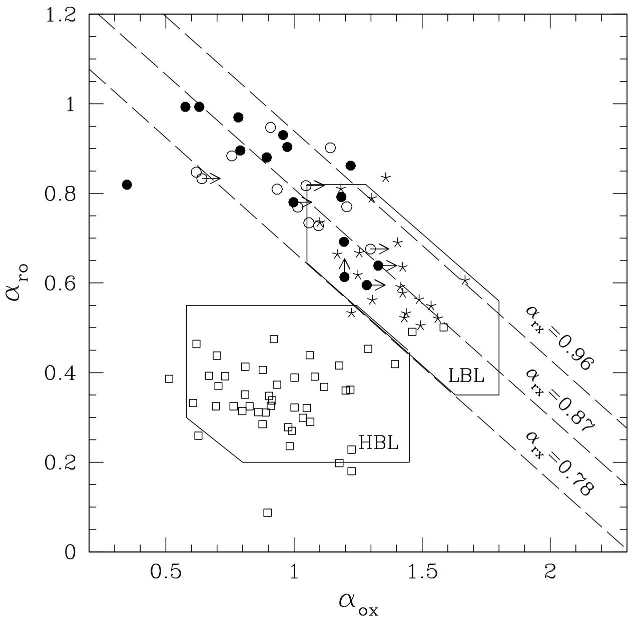

Fig. 10. Broad band spectral indices, calculated between 5 GHz, 5500 Å and 1 keV, for core galaxies (filled circles), low luminosity 3C/FR I radio-galaxies (empty circles), Low energy peaked BL Lacs (stars) and High energy peaked BL Lacs (squares). Solid lines mark the regions within 2 σ from the mean α_{ro} and α_{ox} for BL Lacs drawn from the DXRB and RGB surveys. The dashed lines represent constant values for the third index, α_{rx}.

same comparison [8] including CoreG, see Fig. 10. We considered the radio selected BL Lacs sample derived from the 1Jy catalog (Stickel et al. 1991) and the BL Lac sample selected from the *Einstein* Slew survey (Elvis et al. 1992; Perlman et al. 1996). We used the classification into High and Low energy peaked BL Lacs (HBL and LBL respectively), as well as their multiwavelength data given by Fossati et al. (1998). We also report the regions (solid lines) of the plane within 2 σ from the mean α_{ro} and α_{ox} for the BL Lacs drawn from the Deep X-Ray Radio Blazar Survey (DXRBS) and the ROSAT All-Sky Survey-Green Bank Survey (RGB) (Padovani et al. 2003).

Core galaxies are found to be located in the same region covered by LLRG. This is not surprising since they extend the behaviour of LLRG in the radio/optical and radio/X-ray planes, following Log-Log linear correlations whose slope is close to unity, implying only a small dependence of spectral indices on luminosity. More importantly, they populate the same area in which LBL are found.

We also compared the spectral indices of the different groups taking into account the extended radio-luminosity L_{ext} (see Fig. 11) which does not depend on orientation. This enables us to properly relate objects from the same region of the luminosity function of the parent population. Indeed, the strongest evidence in favour of the FR I/BL Lac unifying model comes from the similarity in the power and morphology of the extended radio emission of BL Lacs and FR I (see e.g. Antonucci & Ulvestad 1985; Kollgaard et al. 1992; Murphy et al. 1993).

The CoreG reach radio-luminosities ∼ 100 smaller than in LLRG and the 1 Jy LBL. In addition, in 13 CoreG the available radio-maps do not allow us to separate core and extended radio-emission and L_{ext} must be considered as an upper limit. This suggests that the CoreG represent the counterparts of the large low luminosity population of BL Lac of LBL type which is now emerging from the low radio flux limit surveys such as the DXRBS (Landt et al. 2001). Clearly, this still requires measurements of the extended radio-luminosity of these low power BL Lac. A ramification of this possible extension of the unified model toward lower luminosities would be the presence of relativistic jets also in our sample of quasi-quiescent early-type galaxies, as this is a prerequisite to produce a substantial dependence of the luminosity on the viewing angle.

We did not find any CoreG with spectral properties similar to those of the High energy peaked BL Lac (HBL), even though HBL have extended radio-emission values of L_{ext} similar to CoreG. The spectral indices of CoreG imply a difference in both the radio-to-optical and radio-to-X-ray flux ratios of an average factor of ∼100 with respect to HBL. The same result applies to LLRG, as all have a LBL-type SED, with the only exception of 3C 264 (Capetti et al. 2000). Our optical selection criteria did not exclude the parent population of HBL since their host galaxies are early-type sufficiently luminous ($M_R < -22.5$, Scarpa et al. 2000) to be included in our sample. Most likely, the dearth of HBL-like CoreG is induced by the radio threshold. Purely radio selected samples of BL Lacs are known to strongly favour the inclusion of LBL; e.g. in the 1 Jy sample there are only 2 HBL out of 34 objects (Giommi & Padovani 1994).

8. Summary and conclusions

The aim of this series of papers is to explore the classical issue of the connection between host galaxies and AGN, in the new light shed by the recent developments in our understanding of the nuclear regions of nearby galaxies.

We thus selected a samples of nearby early-type galaxies comprising 332 objects. We performed an initial selection of AGN candidates requiring a radio detection above ∼1 mJy leading to a sub-sample of 112 sources. Archival HST images enabled us to classify 51 of them into core and power-law galaxies on the basis of their nuclear brightness profile. We here focused on the 29 core galaxies.

---

sion, but it also causes a shift in frequency of the spectral energy distribution (see Chiaberge et al. 2000; Trussoni et al. 2003)

[8] We used the standard definition of spectral indices, measured between 5 GHz, 5500 Å and 1 keV. Optical fluxes have been converted from 8140 Å to 5500 Å using a local slope of $\alpha = 1$; 1 keV fluxes are directly derived from the spectral fit.

We used HST and Chandra archival data to isolate their nuclear emission in the optical and X-ray bands, thus enabling us (once combined with the radio data) to study the multiwavelength behaviour of their nuclei. The detection rate of nuclear sources is 18/29 in the optical (62 %, increasing to 72% if the sources affected by large scale dust are not considered) and 14 in the X-ray, out of the 21 objects with available Chandra data (67 %). Our selection criteria required a radio detection in order to select AGN candidates; 26 CoreG are confirmed as genuine active galaxies based on the presence of i) an optical (or X-ray) core, ii) a AGN-like optical spectrum, or iii) radio-jets, with only 3 exceptions, namely UGC 968, UGC 7898 and NGC 3268.

The most important result of this analysis is that "core" galaxies invariably host a radio-loud nucleus. The radio-loudness parameter R for the nuclei in these sources is on average Log R $\sim$ 3.6, a factor of 400 above the classical threshold between radio-loud and radio-quiet nuclei. The X-ray data provide a completely independent view of their multiwavelength behaviour leading to the same result, i.e. a large X-ray deficit, at the same radio luminosity, when compared to radio-quiet nuclei.

Considering the multiwavelength nuclear diagnostic planes, we found that optical and X-ray nuclear luminosities are correlated with the radio-core power, reminiscent of the behaviour of low luminosity radio-galaxies. The inclusion of CoreG indeed extends the correlations reported for LLRG toward much lower power, by a factor of ~ 1000.

The available radio maps show that in 17 CoreG the extended radio morphology is clearly indicative of a collimated outflow, in the form of either double-lobed structures or jets, although in several cases this can only be seen in high resolution VLBI images. This finding, combined with the analogy of the nuclear properties, leads us to the conclusion that miniature radio-galaxies are associated with all core galaxies of our sample.

The similarity between CoreG and classical low luminosity radio-galaxies extends to other properties. Recent results show that LLRG are always hosted by early-type galaxies with a shallow cusp in their nuclear profile, and this is the case, by definition, for our CoreG. While the distributions of black hole masses, M_{BH}, of the two classes are indistinguishable, hosts of 3C/FR I radio-sources are on average slightly more luminous than CoreG but there is a substantial overlap between the two groups. CoreG and LLRG also share similar properties from the point of view of their emission lines, as all sources with available data conform to the definition of a LINER on the basis of the optical line ratios and they follow a common dependence of line luminosity with radio core power. CoreG and LLRG thus appear to be drawn from the same population of early-type "core" galaxies. They host active nuclei with the same multiwavelength characteristics despite covering a range of 6 orders of magnitude in luminosity. Thus LLRG represent the tip of the iceberg of (relatively) high luminosity objects.

It is unclear what mechanism is driving the level of nuclear activity. As noted above, there is a marginal difference (less than 1 mag) in the host galaxies of CoreG and LLRG; this reflects the well known (but as yet unexplained) trend for which a brighter galaxy has a higher probability of being a stronger radio emitter. As described in Paper I, this effect is present also within our sample of CoreG but it cannot be simply described as a correlation between L_r and M_K.

We explored if there is a relationship between the black hole mass and the radio-luminosity. Again, a very large range of radio-power corresponds to a given M_{BH}. We do not find any relationship between radio-power and black hole mass, clearly indicating that parameters other than the black hole mass play a fundamental role in determining the radio luminosity of a galaxy. No sources with $M_{BH} < 10^8 M_\odot$ are found. However, this might be due to a bias induced by the sample's selection criteria. The limit in optical magnitude translates into a threshold of accessible black hole masses. Only by extending this study to a sample of less luminous galaxies (harbouring, on average, smaller black holes) will it be possible to test the reality of a minimum black hole mass to produce a radio-loud nucleus.

Our data can also be used to set constraints on the radiative manifestation of the accretion process. The nuclear luminosities of CoreG correspond, in units of the Eddington luminosity, to the range $L/L_{\rm Edd} \sim 10^{-6} - 10^{-9}$ in both the optical and X-ray bands. In analogy with the scenario proposed for LLRG, the available data support a common jet origin for the nuclear emission in these observing bands also for CoreG. Thus, the above values should be considered as upper limits to the radiative manifestation of the accretion process, suggesting that accretion occurs both at a low accretion level and at a low efficiency. It is difficult to derive from these results clear constraints on the properties of the accretion flow. In part this is due to the limited information on the Spectral Energy Distribution of the CoreG nuclei and by the fact that in these radio-loud nuclei the observed emission is most likely dominated by radiation from their jets rather than from the accretion. This is further complicated by the presence of several competing accretion models whose predictions of the emitted spectra depend on parameters that are not well constrained by the observations. Nonetheless, in the galaxies with the least luminous nuclei, the estimates of the accretion rate from the literature (derived for the case of spherical accretion), combined with the very low level of X-ray emission, suggest that an important role is played by outflows (or by convection) in order to substantially suppress the amount of gas actually reaching the central object.

As reported above, the CoreG can be effectively considered as miniature radio-galaxies, in terms of nuclear luminosity, thus we are sampling a new region in terms of luminosity for radio-loud AGN. It is interesting to explore the implications of this result also for the model unifying BL Lac objects and radio-galaxies. The broad band spectral indices of CoreG present a very close similarity to those of Low Energy Peaked BL Lac, suggesting the extension of the unified models to these lower luminosities. The CoreG might represent the mis-aligned counterpart of the large population of low luminosity BL Lac emerging from the recent surveys at low radio flux limits. Clearly, a more detailed comparison, taking into account e.g. the (as yet not available) information on the extended radio power and morphology, is needed before this result can be confirmed. An important ramification of this possible extension of the unifying model toward lower luminosities would be the presence of relativistic jets, the essential ingredient of this model, also in our quasi-quiescent early-type galaxies.

In the third paper of the series we will explore the properties of the AGN hosted by galaxies with a power-law brightness profile.

Acknowledgements. This work was partly supported by the Italian MIUR under grant Cofin 2003/2003027534_002. This research has made use of the NASA/IPAC Extragalactic Database (NED) (which is operated by the Jet Propulsion Laboratory, California Institute of Technology, under contract with the National Aeronautics and Space Administration), of the NASA/ IPAC Infrared Science Archive (which is operated by the Jet Propulsion Laboratory, California Institute of Technology, under contract with the National Aeronautics and Space Administration) and of the LEDA database.

References

Antonucci, R. 1993, ARA&A, 31, 473
Antonucci, R. R. J. & Ulvestad, J. S. 1985, ApJ, 294, 158
Auriemma, C., Perola, G. C., Ekers, R. D., et al. 1977, A&A, 57, 41
Balmaverde, B. & Capetti, A. 2005, A&A submitted
Biller, B. A., Jones, C., Forman, W. R., Kraft, R., & Ensslin, T. 2004, ApJ, 613, 238
Blandford, R. D. & Begelman, M. C. 1999, MNRAS, 303, L1
Bondi, H. 1952, MNRAS, 112, 195
Capetti, A. & Balmaverde, B. 2005, A&A, 440, 73
Capetti, A., Kleijn, G. V., & Chiaberge, M. 2005, A&A, 439, 935
Capetti, A., Trussoni, E., Celotti, A., Feretti, L., & Chiaberge, M. 2000, MNRAS, 318, 493
Chiaberge, M., Capetti, A., & Celotti, A. 1999, A&A, 349, 77
Chiaberge, M., Capetti, A., & Macchetto, F. D. 2005, ApJ, 625, 716
Chiaberge, M., Celotti, A., Capetti, A., & Ghisellini, G. 2000, A&A, 358, 104
de Ruiter, H. R., Parma, P., Capetti, A., et al. 2005, A&A, 439, 487
Di Matteo, T., Quataert, E., Allen, S. W., Narayan, R., & Fabian, A. C. 2000, MNRAS, 311, 507
Donato, D., Sambruna, R. M., & Gliozzi, M. 2004, ApJ, 617, 915
Dunlop, J. S., McLure, R. J., Kukula, M. J., et al. 2003, MNRAS, 340, 1095
Elvis, M., Plummer, D., Schachter, J., & Fabbiano, G. 1992, ApJS, 80, 257
Evans, D. A., Kraft, R. P., Worrall, D. M., et al. 2004, ApJ, 612, 786
Fabbiano, G., Elvis, M., Markoff, S., et al. 2003, ApJ, 588, 175
Faber, S. M., Tremaine, S., Ajhar, E. A., et al. 1997, AJ, 114, 1771
Falcke, H., Malkan, M. A., & Biermann, P. L. 1995, A&A, 298, 375
Falcke, H., Nagar, N. M., Wilson, A. S., & Ulvestad, J. S. 2000, ApJ, 542, 197
Ferrarese, L. & Merritt, D. 2000, ApJ, 539, L9
Filho, M. E., Barthel, P. D., & Ho, L. C. 2002, ApJS, 142, 223
Filho, M. E., Fraternali, F., Markoff, S., et al. 2004, A&A, 418, 429
Fossati, G., Maraschi, L., Celotti, A., Comastri, A., & Ghisellini, G. 1998, MNRAS, 299, 433
Franceschini, A., Vercellone, S., & Fabian, A. C. 1998, MNRAS, 297, 817
Gebhardt, K., Bender, R., Bower, G., et al. 2000, ApJ, 539, L13
Giommi, P. & Padovani, P. 1994, MNRAS, 268, L51+
Graham, A. W., Erwin, P., Trujillo, I., & Asensio Ramos, A. 2003, AJ, 125, 2951
Graham, A. W. & Guzmán, R. 2003, AJ, 125, 2936
Henkel, C., Wang, Y. P., Falcke, H., Wilson, A. S., & Braatz, J. A. 1998, A&A, 335, 463
Ho, L. C. 2002, ApJ, 564, 120
Ho, L. C., Feigelson, E. D., Townsley, L. K., et al. 2001, ApJ, 549, L51
Ho, L. C., Filippenko, A. V., & Sargent, W. L. W. 1997, ApJS, 112, 315
Huchra, J., Davis, M., Latham, D., & Tonry, J. 1983, ApJS, 52, 89
Isobe, T., Feigelson, E. D., Akritas, M. G., & Babu, G. J. 1990, ApJ, 364, 104
Jones, D. L. & Wehrle, A. E. 1997, ApJ, 484, 186
Kellermann, K. I., Sramek, R. A., Schmidt, M., Green, R. F., & Shaffer, D. B. 1994, AJ, 108, 1163
Kim, D. & Fabbiano, G. 2003, ApJ, 586, 826
Kollgaard, R. I., Wardle, J. F. C., Roberts, D. H., & Gabuzda, D. C. 1992, AJ, 104, 1687
Kormendy, J. & Bender, R. 1996, ApJ, 464, L119+
Kormendy, J. & Richstone, D. 1995, ARA&A, 33, 581
Kraft, R. P., Forman, W., Jones, C., et al. 2000, ApJ, 531, L9
Krajnović, D. & Jaffe, W. 2002, A&A, 390, 423
Landt, H., Padovani, P., Perlman, E. S., et al. 2001, MNRAS, 323, 757
Lasota, J.-P., Abramowicz, M. A., Chen, X., et al. 1996, ApJ, 462, 142
Lauer, T. R., Ajhar, E. A., Byun, Y.-I., et al. 1995, AJ, 110, 2622
Lauer, T. R., Faber, S. M., Gebhardt, K., et al. 2004,

ArXiv Astrophysics e-prints
Lauer, T. R., Gebhardt, K., Richstone, D., et al. 2002, AJ, 124, 1975
Lewis, K. T., Eracleous, M., & Sambruna, R. M. 2003, ApJ, 593, 115
Loewenstein, M., Mushotzky, R. F., Angelini, L., Arnaud, K. A., & Quataert, E. 2001, ApJ, 555, L21
Maccarone, T. J., Kundu, A., & Zepf, S. E. 2003, ApJ, 586, 814
Mannucci, F., Basile, F., Poggianti, B. M., et al. 2001, MNRAS, 326, 745
Marconi, A. & Hunt, L. K. 2003, ApJ, 589, L21
Murphy, D. W., Browne, I. W. A., & Perley, R. A. 1993, MNRAS, 264, 298
Nagar, N. M., Falcke, H., Wilson, A. S., & Ulvestad, J. S. 2002, A&A, 392, 53
Narayan, R. & Yi, I. 1995, ApJ, 444, 231
Noel-Storr, J., Baum, S. A., Verdoes Kleijn, G., et al. 2003, ApJS, 148, 419
Padovani, P. & Giommi, P. 1995, ApJ, 444, 567
Padovani, P., Perlman, E. S., Landt, H., Giommi, P., & Perri, M. 2003, ApJ, 588, 128
Pellegrini, S. 2005, ApJ, 624, 155
Pellegrini, S., Venturi, T., Comastri, A., et al. 2003, ApJ, 585, 677
Perlman, E. S., Stocke, J. T., Schachter, J. F., et al. 1996, ApJS, 104, 251
Quataert, E. & Gruzinov, A. 2000, ApJ, 539, 809
Randall, S. W., Sarazin, C. L., & Irwin, J. A. 2004, ApJ, 600, 729
Ravindranath, S., Ho, L. C., Peng, C. Y., Filippenko, A. V., & Sargent, W. L. W. 2001, AJ, 122, 653
Rest, A., van den Bosch, F. C., Jaffe, W., et al. 2001, AJ, 121, 2431
Sadler, E. M., Jenkins, C. R., & Kotanyi, C. G. 1989, MNRAS, 240, 591
Satyapal, S., Sambruna, R. M., & Dudik, R. P. 2004, A&A, 414, 825
Scarpa, R., Urry, C. M., Falomo, R., Pesce, J. E., & Treves, A. 2000, ApJ, 532, 740
Schmitt, J. H. M. M. 1985, ApJ, 293, 178
Sérsic, J.-L. 1968, Atlas de Galaxias Australes(Córdoba: Obs. Astron.)
Slee, O. B., Sadler, E. M., Reynolds, J. E., & Ekers, R. D. 1994, MNRAS, 269, 928
Soldatenkov, D. A., Vikhlinin, A. A., & Pavlinsky, M. N. 2003, Astronomy Letters, 29, 298
Stickel, M., Fried, J. W., Kuehr, H., Padovani, P., & Urry, C. M. 1991, ApJ, 374, 431
Terashima, Y. & Wilson, A. S. 2003, ApJ, 583, 145
Tremaine, S., Gebhardt, K., Bender, R., et al. 2002, ApJ, 574, 740
Trinchieri, G. & Goudfrooij, P. 2002, A&A, 386, 472
Trujillo, I., Erwin, P., Asensio Ramos, A., & Graham, A. W. 2004, AJ, 127, 1917
Trussoni, E., Capetti, A., Celotti, A., Chiaberge, M., & Feretti, L. 2003, A&A, 403, 889
Urry, C. M. & Padovani, P. 1995, PASP, 107, 803
Wrobel, J. M. 1991, AJ, 101, 127
Wrobel, J. M. & Heeschen, D. S. 1991, AJ, 101, 148

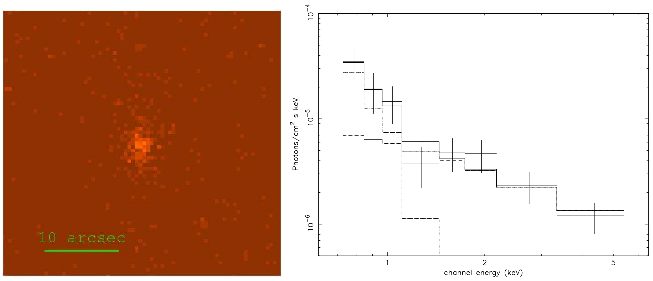

Fig. A.1. Chandra image and spectrum for NGC 3557. The fit and the contributions of the two components (thermal and power-law) are also plotted.

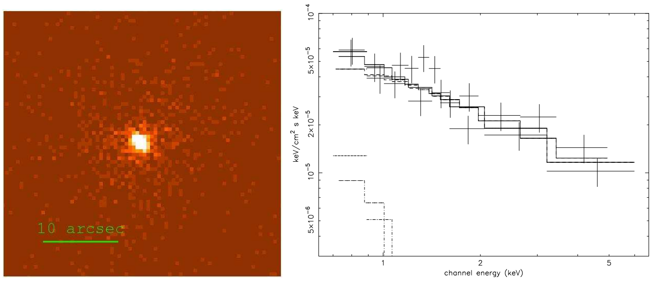

Fig. A.2. Chandra image and spectrum for NGC 5419. The fit and the contributions of the two components (thermal and power-law) are also plotted. Two datasets were fit simultaneously.

Appendix A: Notes on the X-ray observations of the individual sources

We list references and provide comments for the Chandra data and X-ray nuclear measurements found in the literature. We also give images and spectra for the two newly detected X-ray nuclei, as well as a summary of the results of the data analysis which can be found in Table A.1.
UGC 7360: this object is part of the 3C/FR I sample of low luminosity radio-galaxies (3C 270). The Chandra data are presented in Balmaverde & Capetti (2005).
UGC 7386: A total of 310 nuclear counts in 0.2-8 keV band were extracted from a 2″ diameter circle without background subtraction and converted to X-ray luminosity (2-10 keV) assuming an intrinsic power-law spectrum with photon index $\Gamma = 1.8$ and a column density $N_H = 2\ 10^{20}$ cm^{-2} (Ho et al. 2001).
UGC 7494: this object is part of the 3C/FR I sample of low luminosity radio-galaxies (3C 272.1). The Chandra data are presented in Balmaverde & Capetti (2005).
UGC 7629: Both Soldatenkov et al. (2003) and Maccarone et al. (2003) detected emission from the nucleus at energies below 2.5 keV. Biller et al. (2004) confirmed the presence of nuclear emission in the 0.3-10 keV band extracting 64 source counts in an 1″ circle. The spectrum was modeled using a power-law model with photon

Table A.1. Summary of the Chandra data analysis for the two newly detected X-ray nuclei

	Observation information				Fit results				
Name	Obs Id	date	Inst	Exp time	$N_{H,gal}$	Γ	KT	$F_{x,nuc}$(1 keV)	χ^2/d.o.f or PHA bins
NGC 3557	3217	2002-11-28	ACIS-I	40	7.4E20	$1.1^{+0.7}_{-0.8}$	$0.3^{+0.5}_{-0.2}$	$1.1^{+1.0}_{-0.7}E-14$	8
NGC 5419	4999	2004-06-18	ACIS-I	15	5.46E20	$1.9^{+0.6}_{-0.3}$	$0.2^{+1.4}_{-0.1}$	$7.5^{+6.2}_{-1.3}E-14$	17.86/14
	5000	2004-06-19	ACIS-I	15					

index $\Gamma = 1.7$ and a column density $N_H = 1.7\ 10^{20}\mathrm{cm}^{-2}$. These results do not contrast the upper limit given by Loewenstein et al. (2001) who did not find a nuclear component in the hard X-ray band from 2 to 10 keV.

UGC 7654: this object is part of the 3C/FR I sample of low luminosity radio-galaxies (3C 274). The Chandra data are presented in Balmaverde & Capetti (2005).

UGC 7760: Filho et al. (2004) find a bright X-ray nuclear source,spatially coincident with the radio core position. The spectrum of the nuclear source (1200 net counts) is well fitted by a two component model, i.e. a power law ($\Gamma = 1.51$) plus Raymond-Smith thermal plasma (KT=0.95 keV).

UGC 7878: Loewenstein et al. (2001) give a 3 σ upper limit to any nuclear X-ray point source converting the nuclear counts (16 counts in an $1''$ circle region) to luminosity in the 2-10 keV band assuming a power-law spectrum with a slope $\Gamma = 1.5$.

UGC 7898: Soldatenkov et al. (2003) detected nuclear emission at a 3 confidence level only in the range 0.2-0.6 keV with a luminosity of 6 10^{37} erg s^{-1}. Conversely Randall et al. (2004) did not find conclusive evidence for a central AGN. They give an upper limit for the X-ray luminosity converting count rate (0.3-10 keV) into the unabsorbed luminosity L_x(0.3-10 keV) using photon index $\Gamma = 1.78$. We adopted the latter, more conservative, estimate.

UGC 9706: Filho et al. (2004) detected a weak hard x-ray nucleus (total counts) and fitted the spectrum with a power-law model ($\Gamma = 2.29$). Their result is consistent with that of Trinchieri & Goudfrooij (2002).

UGC 9723: Terashima & Wilson (2003) did not detect an X-ray nucleus and suggested that this object is likely to be heavily obscured. They set a nuclear flux upper limit assuming the Galactic absorption column density and a power-law model with photon index $\Gamma = 2$.

NGC 1316: Kim & Fabbiano (2003) detected a low luminosity X-ray AGN; the nuclear spectrum is well reproduced by a power-law model $\Gamma = 1.76$ plus a MEKAL model.

NGC 1399: Loewenstein et al. (2001) did not find a nuclear point source and they give a 3 σ upper limit to any nuclear X-ray point source converting nuclear counts (28 counts in an $1''$ circle region) to luminosity in (2-10 keV band) assuming a slope 1.5 power-law spectrum .

NGC 4696: Satyapal et al. (2004) extracted 39 events in the 2-10 keV band with a $2''$ radius centered on the nucleus and converted to 2-10 keV X-ray luminosity assuming an intrinsic power-law spectrum with $\Gamma = 1.8$ and a Galactic column density.

NGC 5128: In Kraft et al. (2000) the nuclear spectrum is modeled assuming a power-law spectrum with a photon index of 1.9 and $N_H = 10^{23}$ cm^{-2}. Evans et al. (2004) compared different nuclear observations of Cen A and confirmed that the spectrum is well fitted by a heavily absorbed power-law model, consistent with the previous observation.

IC 1459: Fabbiano et al. (2003) detected an un-absorbed nuclear X-ray source ($\sim$ 6500 total counts), with a power law slope $\Gamma = 1.88$.

IC 4296: Pellegrini et al. (2003) found point-like and hard X-ray emission, well described by a moderately absorbed ($N_H = 1.1\ 10^{22}\mathrm{cm}^{-2}$) power-law with $\Gamma = 1.48$.

Appendix B: High resolution radio core measurements

In Sect. 3 we presented measurements of the radio core fluxes obtained from observations obtained at higher resolution and/or frequency with respect to the $5''$ resolution data available for the whole sample. Since these data are highly inhomogeneous and given the general agreement with the 5 GHz VLA measurements, we prefer to retain the values from the surveys by Wrobel & Heeschen (1991) and Sadler et al. (1989), but, nonetheless, we always checked that using these estimates for the core fluxes our results are unchanged. Here we give one example, exploring the influence on the correlation between radio and optical nuclear luminosity: the slope of the best fit is increased by only 0.02, thus it is essentially unaffected.

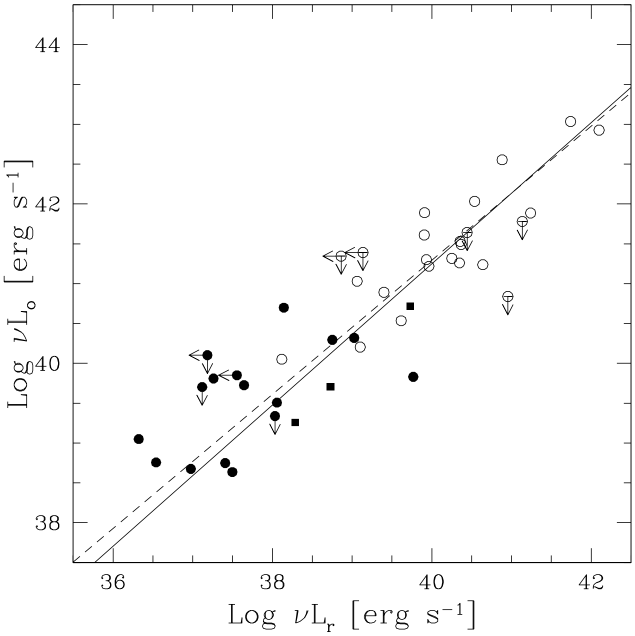

Fig. B.1. Comparison of radio and optical nuclear luminosity for the sample of core-galaxies (filled circles) using the high resolution radio data to measure the radio cores. Empty circles are objects from the 3C/FR I sample of low luminosity radio-galaxies. The dashed line reproduces the best linear fit, while the solid line shows the fits obtained with the 5 GHz VLA data, from Fig. 4.